Metabolism and Chemical Biology

Cancer Research

Targeting Myeloperoxidase Disrupts Mitochondrial Redox Balance and Overcomes Cytarabine Resistance in Human Acute Myeloid Leukemia

Mohsen Hosseini[1,2], Hamid Reza Rezvani[3,4], Nesrine Aroua[1,2], Claudie Bosc[1,2], Thomas Farge[1,2], Estelle Saland[1,2], Véronique Guyonnet-Dupérat[3,4], Sonia Zaghdoudi[1,2], Latifa Jarrou[1,2], Clément Larrue[1,2], Marie Sabatier[1,2], Pierre Luc Mouchel[1,2,5], Mathilde Gotanègre[1,2], Marc Piechaczyk[6], Guillaume Bossis[6], Christian Récher[1,2,5], and Jean-Emmanuel Sarry[1,2]

Abstract

Chemotherapies alter cellular redox balance and reactive oxygen species (ROS) content. Recent studies have reported that chemoresistant cells have an increased oxidative state in hematologic malignancies. In this study, we demonstrated that chemoresistant acute myeloid leukemia (AML) cells had a lower level of mitochondrial and cytosolic ROS in response to cytarabine (AraC) and overexpressed myeloperoxidase (MPO), a heme protein that converts hydrogen peroxide to hypochlorous acid (HOCl), compared with sensitive AML cells. High MPO-expressing AML cells were less sensitive to AraC *in vitro* and *in vivo*. They also produced higher levels of HOCl and exhibited an increased rate of mitochondrial oxygen consumption when compared with low MPO-expressing AML cells. Targeting MPO expression or enzyme activity sensitized AML cells to AraC treatment by triggering oxidative damage and sustaining oxidative stress, particularly in high MPO-expressing AML cells. This sensitization stemmed from mitochondrial superoxide accumulation, which impaired oxidative phosphorylation and cellular energetic balance, driving apoptotic death and selective eradication of chemoresistant AML cells *in vitro* and *in vivo*. Altogether, this study uncovers a noncanonical function of MPO enzyme in maintaining redox balance and mitochondrial energetic metabolism, therefore affecting downstream pathways involved in AML chemoresistance.

Significance: These findings demonstrate the role of myeloperoxidase in the regulation of ROS levels and sensitivity of AML cells to cytarabine, an essential chemotherapeutic backbone in the therapy of AML.

Introduction

Despite a high rate of complete remission after conventional induction chemotherapy, the overall survival is still poor for patients with acute myeloid leukemia (AML), especially in elderly patients. Recent innovative therapies that are FDA-approved or under clinical development, target either particular genetic features such as FLT3-ITD and IDH mutations or specific cellular dependency processes such as BCL2 overexpression and epigenetic modifications (1–6). Furthermore, recent studies have shown several mechanisms of acquired resistance to these molecularly targeted drugs in AML (7–9).

Energy metabolism and redox homeostasis are well-appreciated hallmarks of carcinogenesis and play crucial roles in response to chemotherapy in cancer cells. Several reports emphasize that targeting these features could abolish tumorigenesis and sensitize resistant cells to chemotherapy (10–20). In addition, we and others have recently shown that chemoresistant cells exhibit elevated oxidative phosphorylation (OxPHOS) with imbalanced redox homeostasis (17, 21). Moreover, targeting mitochondrial oxidative metabolism with OxPHOS inhibitors redirects metabolism toward glycolysis and sensitizes resistant cells to cytarabine (AraC) in AML (17, 22). Further studies have also shown that leukemic stem cells (LSC) are characterized by a low rate of energy metabolism with a lower cellular oxidative state and lower basal reactive oxygen species (ROS) production compared with bulk cells (2, 23). These ROS-low LSCs are also unable to upregulate glycolysis after inhibiting OxPHOS, consistent with other reports showing that LSCs have unique mitochondrial characteristics and increased sensitivity to strategies that block OxPHOS (24, 25). Additional studies showed that stem cells reside in a relatively reducing condition (e.g., ROS low), whereas more differentiated cells demonstrate a net increase

[1]Centre de Recherches en Cancérologie de Toulouse, UMR1037, Inserm, Equipe Labellisée LIGUE 2018, Toulouse, France. [2]University of Toulouse, Toulouse, France. [3]INSERM U1035, Bordeaux, France. [4]Université de Bordeaux, Bordeaux, France. [5]Service d'Hématologie, Institut Universitaire du Cancer de Toulouse-Oncopole, CHU de Toulouse, Toulouse, France. [6]Institut de Génétique Moléculaire de Montpellier, University of Montpellier, CNRS, Equipe Labellisée LIGUE, Montpellier, France.

Note: Supplementary data for this article are available at Cancer Research Online (http://cancerres.aacrjournals.org/).

Corresponding Author: Jean-Emmanuel Sarry, Inserm and Université de Toulouse, Oncopole de Toulouse, Toulouse 31024, France. Phone: 335-8274-1632; Fax: 335-6274-4558; E-mail: jean-emmanuel.sarry@inserm.fr

Cancer Res 2019;79:5191–203

doi: 10.1158/0008-5472.CAN-19-0515

in oxidative state (e.g., ROS high). The ROS-low physiologic state can be required by normal and malignant stem cell populations to alleviate both intrinsic and extrinsic stresses and to sustain self-renewal and proliferation potential (26). Finally, because LSCs are more susceptible to changes in ROS content rather normal HSCs, the dysregulation of redox microenvironment will therefore have a greater impact on LSCs.

In this study, we reported that AML cells with an elevated capacity of mitochondrial ($O_2^{\bullet -}$) and cytosolic ROS (H_2O_2) generation are more susceptible to AraC. Moreover, we identified an enhanced myeloperoxidase (MPO) expression and activity in residual leukemic cells (RLC) and in patient-derived xenograft (PDX) with a lower response to AraC *in vivo* as described previously (17). MPO catalyzes the conversion of hydrogen peroxide (H_2O_2) to hypochlorous acid (HOCl). This enzyme is a well-known marker of the myeloid lineage. It is involved in microbicidal function as well as oxidative stress, inflammation, and differentiation (27–30). We further demonstrated that AML cells with higher level of MPO expression rely mainly on mitochondrial metabolism and contain a lower level of toxic oxidants and oxidative damage. Finally, targeting MPO overcomes AraC resistance by altering mitochondrial redox balance and increasing oxidative DNA damage, which consequently impairs OxPHOS metabolism in AML cells. Altogether our findings show that MPO level correlated positively to mitochondrial oxidative and energy metabolism in AML cells and could be employed as a hallmark of chemoresistance to AraC. Finally, this study revealed that MPO plays an important and unexpected role in RLCs beyond its well-known functions in myeloid differentiation and defense.

Materials and Methods

Reagents

AraC was provided by the Pharmacy of Toulouse University Hospital (Toulouse, France). Rotenone, antimycin A, oligomycin, carbonyl cyanide 3 chlorophenylhydrazone, and busulfan were obtained from Sigma-Aldrich. 4-Aminobenzoic acid hydrazide (ABAH) and AZD5904 were supplied by Santa Cruz Biotechnology and MedChem Express, respectively.

Cell lines and culture conditions

Human AML cell lines U937, MOLM-14, MV4-11, HL-60, OCI-AML2, OCI-AML3 (DSMZ), and KG1a (ATCC) were maintained in RMPI1640 medium with GlutaMAX supplement and complemented with 10% FBS (Invitrogen). All cell lines were grown in the presence of 100 U/mL of penicillin and 100 μg/mL of streptomycin, and were incubated at 37°C with 5% CO_2. The cultured cells were split every 2–3 days and maintained in an exponential growth phase. The clinical and mutational features of our AML cell lines are described in Saland and colleagues (31). All cell lines were annually reordered from DSMZ or ATCC stocks and regularly authenticated by morphologic inspection and mutational sequencing and tested negative for *Mycoplasma*. The clinical and mutational features of our AML cell lines are described in Supplementary Table S1.

AML patient samples

Primary AML patient specimens are from Toulouse University Hospital (TUH, Toulouse, France). Frozen samples were obtained from patients diagnosed with AML at TUH after written informed consent in accordance with the Declaration of Helsinki, and stored at the HIMIP collection (BB-0033-00060). According to the French law, HIMIP biobank collection has been declared to the Ministry of Higher Education and Research (DC 2008-307 collection 1) and a transfer agreement was obtained (AC 2008–129) after approbation by ethical committee (Comité de Protection des Personnes Sud-Ouest et Oustremer II). Clinical and biological annotations of the samples have been declared to the CNIL (Comité National Informatique et Libertés ie Data processing and Liberties National Committee). Peripheral blood or bone marrow (BM) samples were frozen in FCS with 10% DMSO and stored in liquid nitrogen. The percentage of blasts was determined by flow cytometry and morphologic characteristics before purification. Samples with >80% blast cell count were chosen for these studies.

Mice xenograft model

Animals were used in accordance to a protocol reviewed and approved by the Institutional Animal Care and Use Committee of Région Midi-Pyrénées (France). NOD/LtSz-scid/IL-2Rγchain^{null} (NSG) mice were produced at the Genotoul Anexplo Platform at Toulouse (France) using breeders obtained from Charles River Laboratory. Mice were housed in sterile conditions using HEPA-filtered micro-isolators and fed with irradiated food and sterile water. Transplanted mice were treated with antibiotic (baytril) for the duration of the experiment. Mice (6–9 weeks old) were sublethally treated with busulfan (30 mg/kg) 24 hours before injection of leukemic cells. Leukemia samples were thawed at room temperature, washed twice in PBS, and suspended in Hank's Balanced Salt Solution (HBSS) at a final concentration of 2 million cells for cell line–derived xenograft model (CLDX) and 10 million cells for PDX model per 200 μL of HBSS per mouse for tail vein injection. Daily monitoring of mice for symptoms of disease (ruffled coat, hunched back, weakness, and reduced mobility) determined the time of killing for injected animals with signs of distress. If no signs of distress were seen, mice were initially analyzed for engraftment 8 weeks after injection except where otherwise noted.

Assessment of leukemic engraftment

Peripheral blood was obtained at the time of injection (day 0) and at the time of dissection (day 8) 2 days after the last dose of AraC to determine the fraction of human blasts using flow cytometry (panel described below). NSG mice were humanely euthanized in accordance with European ethic protocols. BM (mixed from tibias and femurs) and spleen were dissected in a sterile environment and flushed in HBSS with 1% FBS. Mononuclear cells from peripheral blood, BM, and spleen were labeled with FITC-conjugated anti-hCD3, PE-conjugated anti-hCD33, PerCP-Cy5.5-conjugated anti-mCD45.1, APC-conjugated anti-hCD45, and PeCy7-conjugated anti-hCD44 [all antibodies from BD Biosciences, except FITC-conjugated anti-hCD3 from (BioLegend)] to determine the fraction of human blasts ($hCD45^+hCD33^+mCD45.1^-$ cells) using flow cytometry. Analyses were performed on a Becton Dickinson (BD Biosciences) Life Science Research II (LSR II) flow cytometer with DIVA Software (BD Biosciences). The number of AML cells/μL peripheral blood and number of AML cells in total cell tumor burden (in BM and spleen) were determined by using CountBright Beads (Invitrogen) using described protocol.

Cytarabine treatment

Following the mice engraftment (tested by flow cytometry on peripheral blood after 8–18 weeks for PDX and after 2–3 weeks for CLDX), we started to treat them with daily intraperitoneal injections of 30 mg/kg AraC for 5 days (kindly provided by the Pharmacy of the TUH). The *in vivo* experiments were performed in NSG recipients transplanted. For negative control, NSG mice were treated daily with intraperitoneal injection of vehicle for 5 days, PBS 1×. Mice were monitored for toxicity and provided with nutritional supplements as needed.

Measurement of ROS content, mitochondrial membrane potential, and mitochondrial mass

Total HOCl, cytosolic H_2O_2, mitochondrial $O_2^{\bullet-}$ content, mitochondrial membrane potential, and mitochondrial mass were quantified by flow cytometry using R19-S, CM-H2DCF-DA, MitoSox, TMRE, and MitoTracker Green probes, respectively, in viable human $CD45^+CD33^+$ blasts. Of note, R19S exhibits high selectivity for HOCl over other ROS, CM-H_2DCF is oxidized by cytoplasmic ROS to the highly green fluorescent CM-DCF compound, and MitoSOX is targeted to the mitochondria and oxidized by superoxide to a red fluorescence component.

8-OHdG ELISA assay

Total DNA was purified from AML cells by using DNeasy Blood and Tissue Kit (Qiagen). 8-OHdG levels in AML cells were made using 8-OHdG ELISA Kit (Abcam). Colorimetric measurement of 8-oxo levels was provided by using Furostar Optima software. The mean ± SEM of 8-OHdG levels in each cell line was calculated.

Measurement of MPO activity

MPO activity in AML cells was measured using the MPO Assay Kit (ab105136; Abcam), according the manufacturer's instructions. One unit of MPO is defined as the amount of MPO, which hydrolyses the substrate and generates taurine chloramine to consume 1.0 μmol/L of TNB2-probe per minute at 25°C.

Statistical analyses

We assessed the statistical difference between two sets of data using nonparametric *t* test with Welsh correction (GraphPad Prism, GraphPad). Results are expressed as mean ± SEM. Differences were considered as significant for $P<0.05$. *, $P < 0.05$; **, $P < 0.01$; ***, $P < 0.001$.

Results

Low response to cytarabine *in vivo* correlates with lower ROS generation capacity and higher MPO expression

Redox homeostasis is a key regulator of the chemotherapeutic response in cancer cells and altered ROS levels are often observed in drug-resistant cells, suggesting greater capacity to regulate ROS production and to survive in presence of a higher ROS level (32). To determine whether this specific redox buffer capacity and ROS levels are preexisting features that persist through AraC treatment, we have measured cytosolic and mtROS (H_2O_2, HO, and $O_2^{\bullet-}$) levels in AML cells *in vivo* from 20 PDX and two CLDX models (Supplementary Table S1). Thus, AML cells from patients or cell lines were xenografted into NSG-immunodeficient mice as described in Saland and colleagues (31) and Farge and colleagues (17). After disease establishment, mice were treated either with AraC or vehicle (PBS) for 5 days and BM was collected to quantify the reduction in engraftment level and total cell tumor burden. Intracellular cytosolic (H_2O_2) and mitochondrial ($O_2^{\bullet-}$) ROS levels were assessed 2 days following the last dose of AraC in viable (Annexin V^-/7-AAD$^-$) human AML ($CD45^+CD33^+$) cells in BM cells using CM-H2DCFDA and MitoSOX probes, respectively. Results showed that, following AraC treatment, cytosolic and mitochondrial ROS (mtROS) levels were higher in AML patient samples and cell lines that were high responders compared with low responders to AraC *in vivo* in PDX and CLDX models (Fig. 1A and B). This suggests that a higher ROS generation capacity might favor response to AraC in AML cells.

Next, gene set enrichment analysis (GSEA) indicated that the ROS metabolism gene signature [96 genes from gene ontology (GO) database] was enriched in transcriptomes of primary AML patient samples at diagnosis that were low responders to AraC *in vivo* (GSE97393) and in viable residual human AML blasts purified from BM of NSG mice treated with AraC (GSE97631; Fig. 1C). This suggests that lower ROS levels in residual AML cells post-AraC treatment are associated with genes implicated in ROS metabolism in AML cells before treatment. Datamining analyses of upregulated genes in both AraC-resistant AML blasts and in low responder patients revealed enrichment in genes involved in biological pathways such as cellular proliferation, immune response, and response to oxidative stress (Supplementary Fig. S1A; Supplementary Table S2). Focusing on genes implicated in ROS metabolism, we found that 27 genes were upregulated in AraC residual cells *in vivo* and 11 genes upregulated at diagnosis in patients with a low response to AraC (Supplementary Fig. S1A). Comparing these two specific ROS gene signatures with a GO-curated ROS gene signature, Venn diagrams showed only one common upregulated gene, *MPO*, myeloperoxidase, implicated in response to oxidative stress (Fig. 1D). *MPO* mRNA expression was indeed significantly higher in AML patient samples (17) and cell lines (4) that were low responder *in vivo* to AraC compared with high responders *in vivo* (Fig. 1E; Supplementary Table S1). Although *MPO* mRNA expression was heterogeneous in AML, it was also higher in both complex and normal karyotypes compared with normal hematopoietic stem cells (HSC; cohort BloodPool; Fig. 1F). Surprisingly, *MPO* expression was negatively correlated to NPM1 mutation, which is considered as a favorable prognosis in AML (Fig. 1G), and to M5 subgroup (Supplementary Fig. S1B). These data suggest that targeting MPO in some AML patient subtypes such as the ones harboring NPM1 mutations or M5-FAB is due to a better response to AraC. Consistent with these data, Brunetti and colleagues have recently reported that depletion of cytoplasmic NPM1 significantly increased CD11b, CD14, and MPO expression through downregulation of homeobox genes in NPM1-mutant AML cell lines (33). Taking advantage of this MPO expression heterogeneity in AML patient samples, we have generated gene signatures from three independent publicly accessible cohorts [Verhaak (34), Metzeler (35), and the Cancer Genome Atlas (TCGA)] of AML patient samples with the highest MPO expression compared with the lowest MPO expression, hereinafter called *MPO* gene signature, that include 101 genes, 111 genes, and 100 genes, respectively (Supplementary Fig. S1C). GSEA analysis showed that this specific MPO gene set is enriched in both patients with lower response to AraC *in vivo* and AraC-treated residual cells *in vivo* (Fig. 1H and I, respectively) and enriched in patients at relapse compared with diagnosis (Fig. 1J). Altogether, these results indicate that resistance to AraC is positively associated with high MPO expression in AML cells.

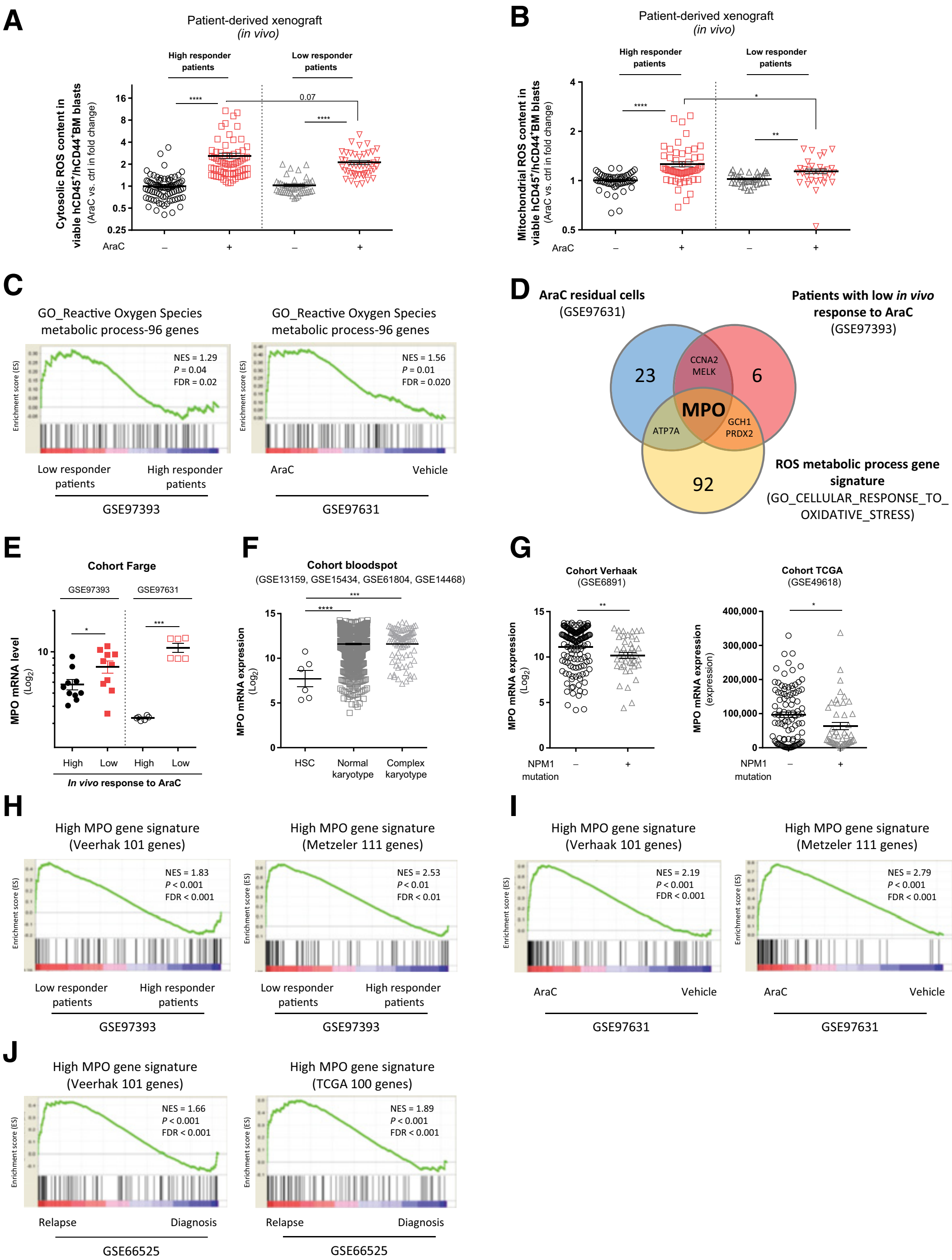

Figure 1.

In vivo response to cytarabine is correlated with ROS generation capacity and MPO expression in AML. **A,** Intracellular ROS levels were measured by CM-H2DCFDA labeling in human viable (Annexin V^-/7-AAD$^-$) CD45$^+$CD33$^+$ AML cells from AraC- versus vehicle (PBS)-treated mice xenografted with AML cell lines and patient cells that have high or low response (threshold, 10-fold reduction) to AraC *in vivo*. Each dot corresponds to mean fluorescence intensity (MFI) of one mouse. **B,** mtROS level was evaluated by MitoSOX probe in human viable (Annexin V^-/7-AAD$^-$) CD45$^+$CD33$^+$ AML cells from AraC- versus vehicle (PBS)-treated mice xenografted with AML patient cells that have high or low response (threshold, 10-fold reduction) to AraC *in vivo*. Each dot corresponds to mean fluorescence intensity of one mouse. **C,** GSEA of ROS gene signature was performed from transcriptomes of patients who are low (red) versus high (blue) responders to AraC *in vivo* or from transcriptomes of residual human AML cells purified from AraC-treated (red) compared with vehicle (PBS)-treated (blue) AML-xenografted mice. Kolmogorov–Smirnov statistical test was performed. **D,** Venn diagram of the overlapping genes enriched in AML residual cells obtained from AraC versus PBS-treated PDX models (GSE97631), in patients with low *in vivo* response to AraC compared with patients with high *in vivo* response to AraC (GSE97393), and in ROS gene signature obtained from curated GO_cellular_response_to_oxidative stress. (*Continued on the following page.*)

Enhanced MPO expression and activity increases resistance to cytarabine and sensitizes to ABAH in AML

Previous studies have demonstrated that MPO promotes oxidative stress through the production of toxic HOCl from H_2O_2 during inflammation and for neutrophil microbial killing activity, and participates in oxidative stress–mediated apoptosis in AML cells (36, 37). It was suggested that ROS-generating agents may serve as an enhancer of chemotherapy via MPO-mediated production of ROS in myeloid leukemic cells (36). Kim and colleagues (37) have demonstrated that AML cells having an elevated level of MPO are more sensitive to parthenolide, a nonspecific ROS-generating compound. However, the role of MPO in AML chemoresistance was not addressed. Therefore, we examined whether high MPO-expressing cells are more resistant to AraC and more vulnerable to MPO inhibitors. We first assessed expression and activity of MPO in four diverse AML cell lines. AML cell lines with higher MPO protein and mRNA expression level (Fig. 2A and B) were enriched in MPO gene signatures generated from Verhaak (34), Metzeler (35), and TCGA databases, respectively (Fig. 2C; Supplementary Fig. S1D). Of note, AML cell lines selectively overexpressed *MPO* mRNA among all cancer cell lines (Cancer Cell Line Encyclopedia from the Broad Institute; Supplementary Fig. S1E). Moreover high MPO cell lines also had an elevated level of MPO activity (Fig. 2D) and treatment with ABAH, an irreversible and specific inhibitor of MPO activity, resulted in significant reduction of MPO activity in high MPO-expressing AML cell lines (Fig. 2D). Finally, high MPO-expressing AML cells were more sensitive to ABAH compared with low MPO-expressing cells *in vitro* (Fig. 2E).

Next, we selected two AML cell lines with two different levels of MPO expression, namely MOLM-14 (as high MPO cell line) and U937 (as a low MPO cell line). Although HL60 presented higher MPO activity (Fig. 2D), MOLM14 was used over HL60 because of its higher level of engraftment in mice. We injected U937 or MOLM14 in adult NSG mice, treated AML-xenografted mice with PBS or AraC, and then sorted viable human AML blasts from BM to assess their respective EC_{50} for the MPO inhibitor (ABAH) *ex vivo* (Fig. 2F). Furthermore, we found that EC_{50} for ABAH in sorted human AML cells from PBS- or AraC-treated PDX models ($n = 5$; Supplementary Table S1) was significantly reduced in AraC-residual cells compared with PBS-treated cells (Fig. 2G). On the basis of the fluorescence of the HOCl-dependent redox dye R19-S, we sorted and purified human AML cell subpopulations with high versus low HOCl content from *in vitro* MOLM14 and CLDX models *in vivo* (Fig. 2H). This revealed that subfractionated AML cells with high HOCl content (e.g., high ABAH-sensitive MPO activity; Fig. 2I) overexpressed *MPO* mRNA (Fig. 2J) and were more resistant to AraC and more sensitive to ABAH compared with subfractionated AML cells with low HOCl content *in vivo* and *in vitro* (Fig. 2K and L). These data strongly suggest that MPO upregulation or an increase in HOCl content contributes to the resistance of AML cells to AraC.

Elevated MPO activity is associated with alterations in both ROS metabolism and energetic balance in AML

ROS homeostasis and signaling plays a crucial role in AML response to treatment (2, 17, 38, 39). In particular, ROS are known to be critical mediators of genotoxic-induced cell death, even though their cellular effectors are still ill-defined (40, 41). In this context, we have previously shown a novel role for ROS in AML cell response to chemotherapeutic drugs through the inhibition of the SUMOylation pathway (42). As MPO is one of the key (but understudied) components of ROS metabolism (Fig. 3A), we next examined whether MPO would impact ROS metabolism in AML *in vitro* and *in vivo*. We measured cytosolic (H_2O_2) and mitochondrial ($O_2^{\bullet -}$) ROS content in residual AML cells following transplantation of low MPO-expressing U937 and high MPO-expressing MOLM14 cells into immunodeficient mice and treatment with vehicle and AraC. Results showed that the increase in cytosolic and mtROS levels in AraC-residual cells are lower in high MPO-expressing CLDX model compared with low MPO-expressing CDLX model in response to AraC chemotherapy *in vivo* (Fig. 3B and C). Because we have already shown that U937 and MOLM14 cells are, respectively, classified as low and high responder cell lines to AraC treatment (17), these results indicate that the Low MPO-expressing U937 cells that produced higher level of ROS are more sensitive to chemotherapy (Supplementary Fig. S2A–S2C). Importantly, HOCl content was elevated after AraC treatment in high MPO-expressing MOLM-14 cells *in vivo* (Fig. 3D). Accordingly, we concluded that AML cells with a higher capacity of ROS (especially mtROS, i.e., superoxides) generation are more responsive to AraC *in vivo*.

Under physiologic conditions, mtROS production and detoxification are tightly balanced. Impairment of this equilibrium enables mtROS to induce a diverse array of signaling networks such as intracellular signaling associated with a metabolic switch toward Warburg phenotype, inflammation, differentiation, cellular damage, and cell death (43–46). Here, we determined whether MPO might influence mitochondrial and OxPHOS metabolism in AML. First, GSEA showed an enrichment in high OXPHOS gene signature (17) in AML patient samples with high MPO expression obtained from three independent patient transcriptomic databases (Fig. 3E). The gene signature was generated through our previous work (17) from low and high OxPHOS AML cell lines (defined as low and high mitochondrial ATP-producing and mitochondrial oxygen–consuming AML cell lines). To functionally confirm this and to better understand the relationship between MPO expression, OxPHOS metabolism and mtROS generation, we measured the energetic balance, HOCL content, and mtROS in MOLM14 cells in presence of ABAH and AraC.

(*Continued.*) **E,** Comparison of *MPO* mRNA expression in AML patient samples (GSE97393) and cell lines (GSE97631) with high versus low responder to AraC. **F,** Bloodspot transcriptomic database was used to compare *MPO* mRNA expression in human AML cells with complex or normal karyotypes to normal HSCs from healthy donor. **G,** Correlation of *MPO* mRNA expression in NPM1 wild-type and -mutated AML cells from GSE6891 and GSE49618 cohorts. **H,** GSEA of two high *MPO* gene signatures obtained from GSE6891 and GSE12417 transcriptomic databases was performed from transcriptomes (GSE97393) of low (red) versus high (blue) responder AML patient samples. Kolmogorov–Smirnov statistical test was performed. **I,** GSEA of two high *MPO* gene signatures obtained from GSE6891 and GSE12417 transcriptomic databases was performed from transcriptomes (GSE97631) of residual AML cells purified from AraC-treated (red) compared with vehicle (PBS)-treated (blue) AML-xenografted mice. Kolmogorov–Smirnov statistical test was performed. **J,** GSEA of two high *MPO* gene signatures obtained from GSE6891 and GSE49618 transcriptomic databases was assessed from transcriptomes of patients in relapse (red) versus patients in diagnosis (blue). Kolmogorov–Smirnov statistical test was performed. Graphs of mean ± SEM. *P* values were determined by Welch correction test (**A**, **B**, **E**, **F**, and **G**). n.s., not significant; *, $P \leq 0.05$; **, $P \leq 0.01$; ***, $P \leq 0.001$; ****, $P < 0.0001$.

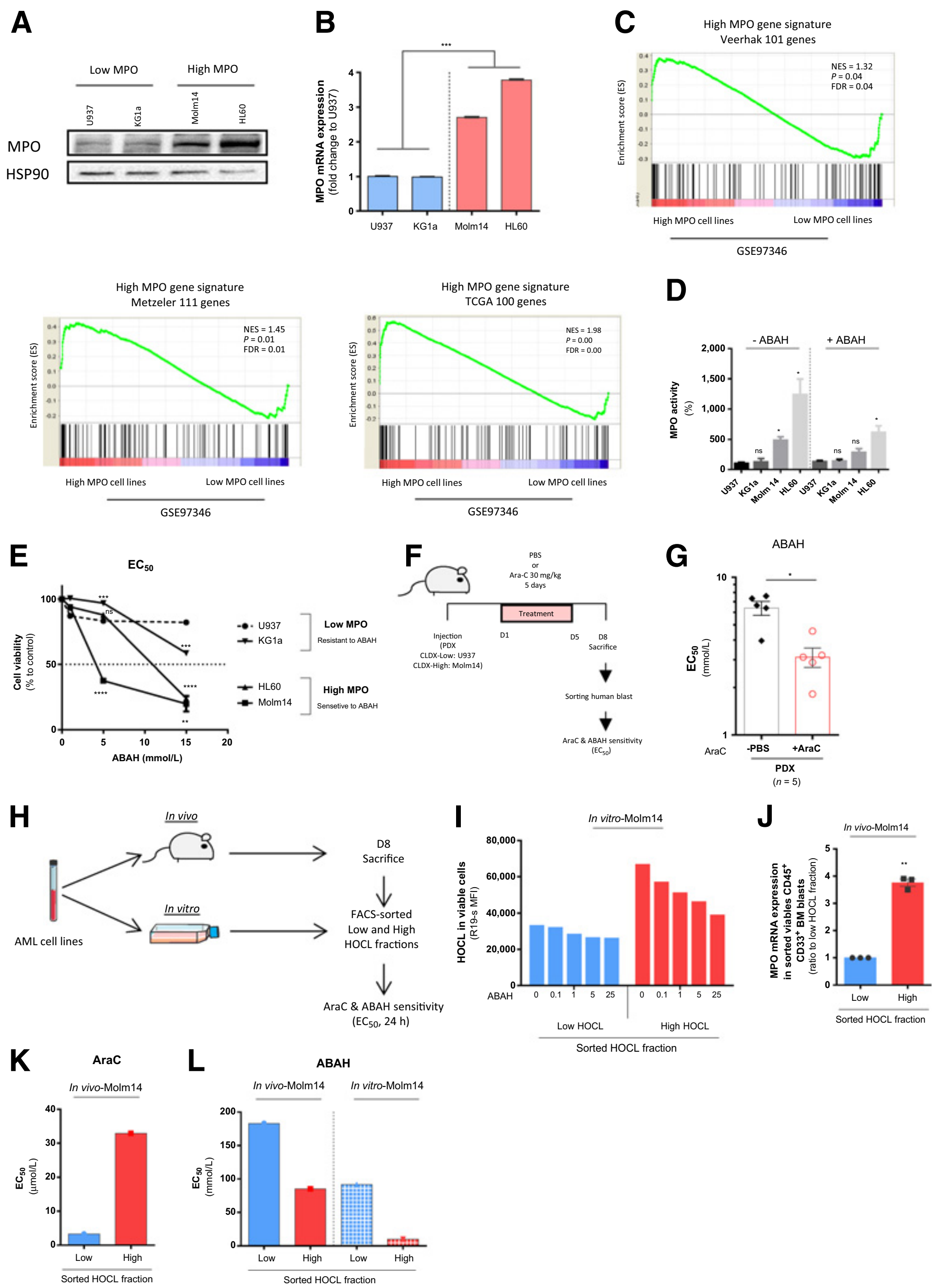

Figure 2.

Enhanced MPO expression and activity increases resistance to cytarabine and sensitizes to the MPO inhibitor, ABAH, in AML. **A,** Western blot analyses of MPO protein level in low versus high MPO AML cell lines. **B,** RNA quantification of MPO in low and high MPO AML cell lines. **C,** GSEA of three high *MPO* gene signatures obtained from GSE6891, GSE12417, and GSE49618 AML patient databases was performed from transcriptomes (GSE97346) of human high (red) versus low (blue) MPO cell lines. Kolmogorov–Smirnov statistical test was performed. **D,** MPO activity was measured in four diverse AML cell lines in absence or presence of MPO-specific inhibitor, ABAH. Results were normalized to U937. **E,** *In vitro* EC_{50} for 24 hours of ABAH in AML cell lines normalized to their matched PBS-treated AML cell lines. **F,** Experimental design of the chemotherapy treatment used *in vivo* in AML cell line- or patient-xenografted mice. Mice were then treated with PBS or AraC (30 mg/kg/day) for 5 days and were sacrificed at day 8 and then viable residual AML blasts were FACS sorted. **G,** Human residual AML cell lines sorted from mice BM were treated *ex vivo* with ABAH for 24 hours and their EC_{50} was calculated and compared with EC_{50} from matched PBS-treated AML cells. **H,** Experimental design of the *in vivo* MOLM14-xenografted mice and *in vitro* MOLM14 assays to sort high HOCl and low HOCl cells using RS-19 probe. **I,** *Ex vivo* sensitivity of low and high HOCl-sorted fractions to ABAH was evaluated after 24 hours by RS-19 labeling. **J,** mRNA expression of MPO in low and high HOCL fractions. *Ex vivo* treatment of both sorted fractions with AraC (**K**) or ABAH (**L**) for 24 hours and calculation of their respective EC_{50}. Graphs of mean ± SEM. *P* values were determined by Welch correction test (**B**, **D**, **E**, **G**, **H**, **I**, **K**, and **L**). n.s., not significant; *, $P \leq 0.05$; **, $P \leq 0.01$; ***, $P \leq 0.001$; ****, $P < 0.0001$.

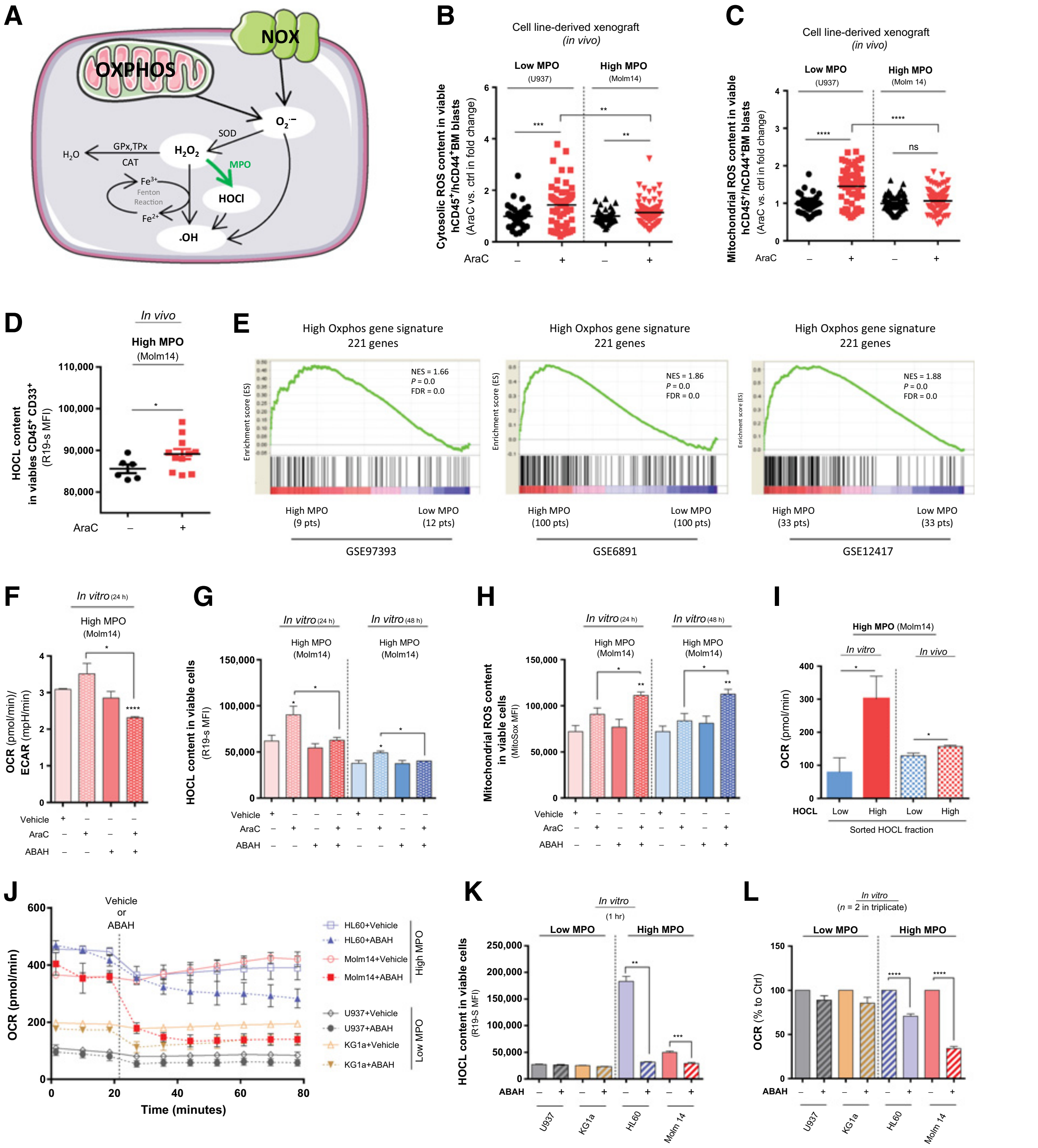

Figure 3.

Elevated MPO expression is associated with alterations in both ROS metabolism and energetic balance, and MPO inhibition disrupts mtROS and energetic metabolisms in AML. **A,** Schematic diagram of ROS metabolism in AML cells. **B,** Intracellular ROS levels were measured by CM-H2DCFDA in human viable (Annexin V^-/7-AAD^-) $CD45^+CD33^+$ AML cells from AraC- versus vehicle (PBS)-treated mice xenografted with low (U937) versus high (Molm14) MPO cell lines. Each plot corresponds to mean fluorescence intensity (MFI) of each mouse. **C,** mtROS level was quantified by MitoSOX probe in human viable (Annexin V^-/7-AAD^-) $CD45^+CD33^+$ AML cells from AraC- versus vehicle (PBS)-treated AML-xenografted mice. Each plot corresponds to mean fluorescence intensity of each mouse. **D,** Intracellular HOCl content were measured by RS-19 probe in AraC- versus vehicle (PBS)-treated MOLM14 CLDX model. **E,** GSEA of high OxPHOS gene signature was performed from patients with low (red) versus high (blue) *MPO* expression in three transcriptomic databases (GSE97393, GSE6891, and GSE12417). Kolmogorov–Smirnov statistical test was performed. **F–H,** OCR/ECAR ratio, HOCL content, and mtROS were measured following 24 hours of treatment (AraC at 0.8 μmol/L and ABAH at 1 mmol/L). **I,** Basal OCR of low and high HOCl-sorted fractions from *in vitro* and *in vivo* MOLM14 CLDX model. **J,** Oxygen consumption rates plots of two low versus two high MPO AML cell lines in presence of vehicle or MPO-specific inhibitor, ABAH, as evaluated by the Seahorse XF24 extracellular flux analyzer. **K,** HOCL content was performed 1 hour upon ABAH therapy. **L,** Comparison of basal OCR between treated and untreated cells. Graphs of mean ± SEM. *P* values were determined by Welch correction test (**B**, **C**, **D**, and **F–K**). n.s., not significant; *, $P \leq 0.05$; **, $P \leq 0.01$; ***, $P \leq 0.001$; ****, $P < 0.0001$.

Combined treatment with ABAH and AraC significantly decreased the energetic balance and HOCL content, while it significantly increased mtROS (Fig. 3F–H). Interestingly, purified human AML cell subpopulation with high HOCl content revealed an elevated rate of basal oxygen consumption compared with purified human AML cell subpopulation with low HOCl content in both *in vitro* and *in vivo* from MOLM14 cell lines (Fig. 3I; Supplementary Fig. S3A–S3C) and PDX models (Supplementary Fig. S3D). Furthermore, basal oxygen consumption rate (OCR) and HOCL content in different AML cell lines in the presence of ABAH were quantified by Seahorse analyzer and flow cytometry, respectively (Fig. 3J–L). Surprisingly, we found that *in vitro* ABAH treatment significantly reduced basal OCR and HOCl content in high MPO cell lines compared with low MPO cell lines during the OCR assay (Fig. 3L).

Altogether, these results suggest that elevated levels of MPO are associated with a higher OxPHOS gene phenotype and activities that were previously correlated to resistance to AraC (17, 21, 47). Interestingly, recent studies indicated that elevated level of mtROS could be considered as a hallmark of mitochondrial dysfunction (45, 48) and that mitochondrial selective targeting sensitizes resistant cells to chemotherapy (17, 22, 49). Consistent with these studies, Lagadinou and colleagues (2) characterized the oxidative state of LSCs and suggested mitochondria as the primary site of oxidative metabolism in LSC-enriched populations. We showed here that AML cells with high MPO expression and consequently high HOCl content have an increased mitochondrial oxygen consumption. We further demonstrated that the inhibition of MPO activity in these cells leads to impaired mitochondrial respiration and increased mtROS level, suggesting that excessive mtROS production upon MPO inhibition could be the mechanism underlying the deficiency in mitochondrial metabolism.

MPO inhibition enhances response to cytarabine in AML

Persistent ROS stress may induce adaptive responses, enabling cancer cells to survive with high levels of ROS (50). Recent publications have shown that the leukemic phenotype correlates with elevated ROS levels. In particular, a recent study has demonstrated that AML cells are more susceptible to oxidative stress than normal cells due to a lower spare respiratory capacity, suggesting that pharmacologic interventions aimed at altering ROS levels might reveal a selective antileukemic strategy (25). Further supporting this idea, ROS inducers (e.g., parthenolide, piperlongumine, and arsenic) were shown to preferentially target less abundant AML LSCs, which are responsible for patient relapse due to their intrinsic poor sensitivity to chemotherapeutic drugs and display deregulated redox metabolism (2, 51, 52). Therefore, modulating (up or down) ROS levels can render cancer cells highly susceptible to apoptosis through alterations of both energetic and ROS metabolism. As previous work (17, 21, 47) showed that high OxPHOS cells are resistant to chemotherapies, we asked whether inhibition of MPO could sensitize AML cells to AraC by blocking/inhibiting mitochondrial energetic and oxidative metabolism. To answer this question, U937 and MOLM14 cells were treated with PBS, AraC, ABAH (or AZD5904, another newly available MPO-specific inhibitor), and the combination of ABAH (or AZD5904) and AraC for 24 hours *in vitro*. While no significant change in HOCl level was observed in low MPO-expressing U937 cells, HOCl level was significantly increased in MOLM14 upon treatment with AraC (Supplementary Fig. S4A). AraC-mediated increased HOCl was impaired in the presence of ABAH (Supplementary Fig. S4A). ROS measurement showed that mtROS level was significantly elevated following monotherapy with ABAH and combination therapy in this high MPO cell line (Supplementary Fig. S4B). We also observed a decrease in mitochondrial mass following combination therapy and we have found that the ratio of mtROS to mitochondrial mass indicate an elevated level of mtROS in the combination of MPO inhibitors and AraC compared with AraC alone (Supplementary Fig. S4B–S4D). The cellular energetic balance (OCR/ECAR ratio) was diminished in MOLM14 after treatment with ABAH and under combination therapy (Supplementary Fig. S4E). Subsequently, we found a significant induction of apoptosis (loss of MMP) and a significant reduction of the cell viability upon combination therapy (Fig. 4A and B). Altogether, combining AraC to MPO inhibition resulted in increased mtROS, decreased OCR/ECAR ratio, and consequently induced apoptosis in MOLM14 cells.

MPO silencing increased oxidative damages in response to cytarabine in AML

To further analyze the role of MPO in the resistance to AraC, we generated two short hairpin RNAs against MPO (Fig. 4C; Supplementary Fig. S5A). A significantly marked reduction of HOCl content even upon AraC treatment was observed in shMPO MOLM14 cells (Fig. 4D; Supplementary Fig. S5B and S5C). Depletion of MPO decreased mitochondrial oxygen consumption (Fig. 4E) and the cellular energetic balance (Fig. 4F; Supplementary Fig. S5D), suggesting that MPO has an impact on OxPHOS metabolism. Furthermore, upon AraC treatment, MPO downregulation was associated to higher production of mtROS (Fig. 4G; Supplementary Fig. S5E). It has been shown that excessive production of ROS particularly from the mitochondria is the main cause of oxidative damage (53–57). Therefore, we asked whether increasing mtROS level upon MPO downregulation in AraC-treated cells could be positively associated with an increased oxidative damage. To test this hypothesis, we evaluated the expression level of 8-oxoguanine DNA glycosylase (OGG1), a well-known enzyme involved in the repair of oxidative damage, and quantified 8-oxoguanine (8-oxoG), one of the most common oxidative lesions arising from ROS. Results showed that mRNA expression of H2A histone family, member X (*H2AX*) and *OGG1* were significantly upregulated in shMPO-transduced cells treated with AraC (Fig. 4H and I; Supplementary Fig. S5F). Assessment of Ataxia-telangiectasia–mutated protein (ATM) and phosphorylated H2AX protein level also confirmed their significant overexpression in shMPO-transduced cells treated with AraC (Fig. 4J). Moreover, measurement of 8-oxoG levels showed a marked increase in this biomarker of oxidative DNA damage in MPO-depleted cells upon AraC therapy (Fig. 4K). Datamining analyses on bloodspot cohort showed that *OGG1* RNA expression is significantly lower in AML cells compared with normal HSCs (Supplementary Fig. S6A). Along the same vein, the OGG1 RNA level was lower in xenografts from AML patient samples and cell lines with low response to AraC *in vivo* (Supplementary Fig. S6B). Of note, *OGG1* RNA expression is negatively associated to MPO level (Supplementary Fig. S6C–S6E). Consistently, GSEA showed an enrichment in high *OGG1* gene signature generated from transcriptomic database (GSE14468; ref. 34) in AML patient samples and cell lines with lower response to AraC *in vivo* compared with the ones with higher response to AraC and in patient samples at relapse compared with patients at diagnosis (Supplementary Fig. S6F). Finally, we observed a significant increase in

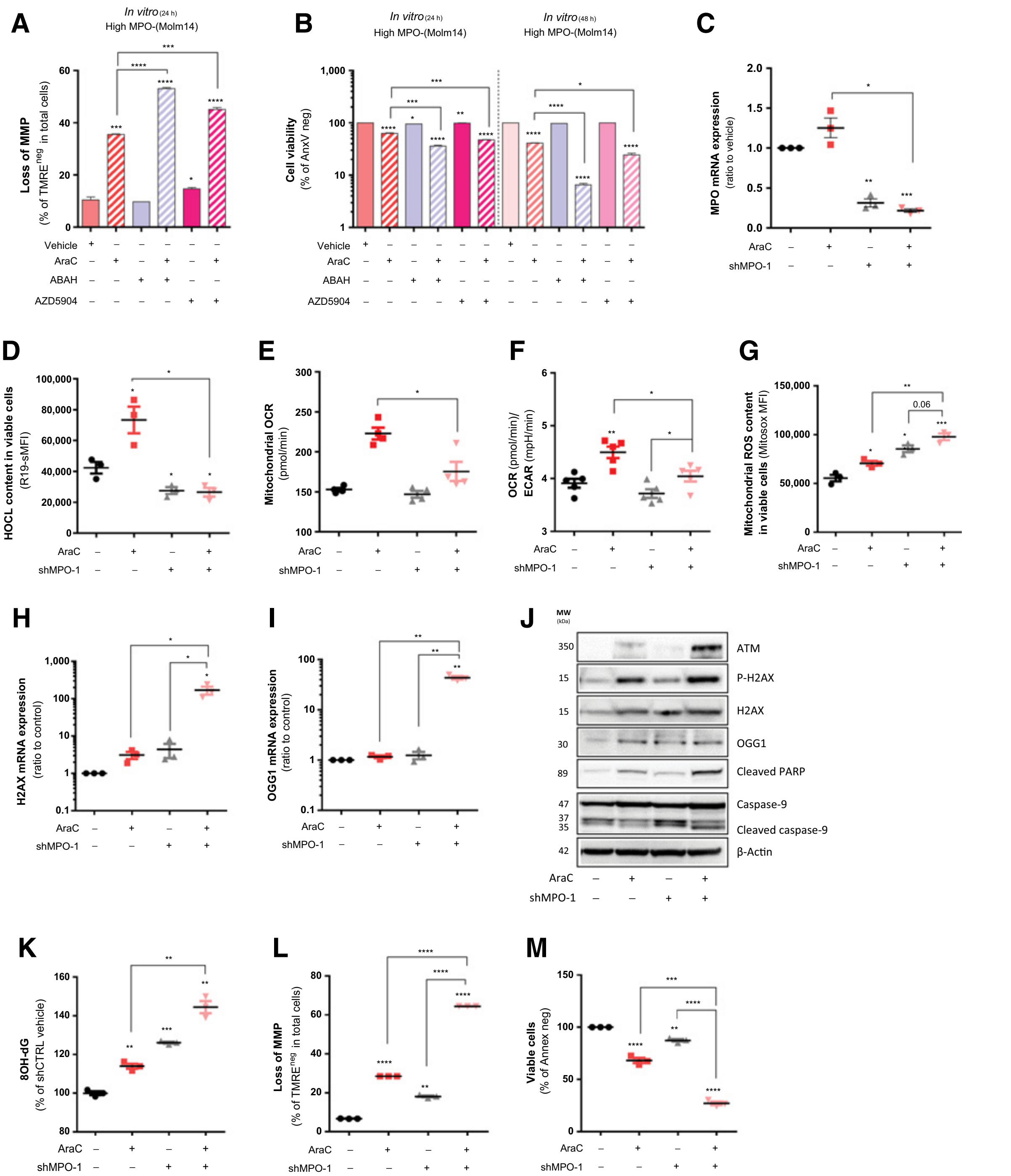

Figure 4.

In vitro MPO downregulation induces mtROS generation along with mitochondrial dysfunction. **A,** Assessment of loss of mitochondrial membrane potential after 24 hours in treated Molm14 by ABAH, AZD5904, and AraC. **B,** Measurement of cell viability upon 24 and 48 hours treatment by ABAH, AZD5904, and AraC. **C,** Quantification of MPO mRNA expression. **D**, HOCl content was measured by R-19S in viable shCtrl versus shMPO-transduced Molm14 upon 24 hours treatment by AraC (0.4 μmol/L). **E** and **F,** Basal respiration and OCR/ECAR ratio was performed by Seahorse analyzer in viable cells. **G,** Evaluation of mtROS by MitoSOx following AraC therapy in viable shCtrl versus shMPO cells. H2AX (**H**) and OGG1 (**I**) mRNA expression of treated and untreated shCtrl versus shMPO cells was performed after 24 hours of AraC therapy. **J,** Western blot analyses of MPO, caspase-9, ATM, phosphorylated H2AX, and H2AX upon 24 hour treatment by AraC in shCtrl versus shMPO-Molm14. **K,** Measurement of 8-oxo level 24 hours following treatment. **L** and **M,** Quantification of loss of mitochondrial membrane potential and viability in shCtrl versus shMPO-transduced cells. Graphs of mean ± SEM. *P* values were determined by Welch correction test (**A–I** and **K–M**). n.s., not significant; *, $P \leq 0.05$; **, $P \leq 0.01$; ***, $P \leq 0.001$; ****, $P < 0.0001$.

PARP and caspase-9 cleavage (Fig. 4J), loss of mitochondrial membrane potential, and a strong reduction of the cell viability in shMPO-transduced AML cells upon AraC treatment (Fig. 4L and M; Supplementary Fig. S6G and S6H). The EC_{50} of shMPO-transduced cells for AraC was significantly decreased *in vitro* while we observed an increase in the EC_{50} for ABAH compared with shCtl-transduced cells (Supplementary Fig. S6I). Because mitochondrial DNA is more susceptible to oxidative damage than nuclear DNA (58), increased mtROS level–mediated oxidative mitochondrial DNA damages in shMPO-transduced cells treated with AraC could result in a deficiency in mitochondrial metabolism that drives their apoptotic death.

Altogether these data confirmed that MPO expression is an important component of the cellular and mitochondrial redox balance. Subsequently alteration of MPO expression affects mtROS level and mitochondrial energy metabolism along with an elevated level of oxidative damages in AraC-treated cells. Finally, MPO inhibition potentiates AraC effect *in vitro*.

In vivo inhibition of MPO therapeutically sensitizes resistant cells to cytarabine

Next, we sought to further examine the role of MPO *in vivo* and to determine whether MPO inhibition could sensitize AML cells to AraC *in vivo*. We injected MPO- and mock-depleted AML MOLM14 cells into adult NSG mice and treated the mice with AraC for 5 days (Fig. 5A). *In vivo MPO* expression was significantly reduced in shMPO-transduced MOLM14 cells in both untreated and treated cells with AraC (Fig. 5B). We also showed a pronounced decrease in HOCl level in human-depleted MPO blasts following AraC therapy *in vivo* (Fig. 5C). As expected, mtROS level was significantly increased in human MPO–depleted cells upon AraC treatment *in vivo* (Fig. 5D). Furthermore, we observed a decrease in basal OCR (Fig. 5E) and an increase in *OGG1* level in sorted MPO-depleted human residual AML cells upon chemotherapy (Fig. 5F). Consistent with our *in vitro* results, loss of mitochondrial membrane potential (e.g., early apoptosis) and reduction in cell viability were observed in both shCLT and shMPO AML cells upon AraC treatment (Fig. 5G and H). Furthermore, the reduction in the total cell tumor burden post-AraC was 2-fold greater in shMPO cells than shCTL MOLM14 cells (Fig. 5H). As MPO primes AML differentiation (29), we assessed the expression of CD11b, as a differentiation marker, and the results showed that MPO silencing significantly reduced the differentiation upon AraC treatment (Supplementary Fig. S7A). Interestingly, inhibition of MPO by shMPO sensitized AML cells to AraC as shown by lower EC_{50} for AraC in shMPO-transduced cells compared with shCTL-transduced cells (Fig. 5I). Of note, these cells were more resistant to ABAH (Fig. 5J). These results confirmed our data obtained using ABAH *in vitro* with both AML cell lines and patient specimens (Supplementary Fig. S7B), and transduced cells by lentiviral shMPO *in vitro*. Finally, *in vivo*, 2-week treatment with MPO inhibitor, AZD5904, significantly enhanced anti-AML effect of AraC (Fig. 5K and L) with an increase in both mtROS production (Supplementary Fig. S7C) and dissipation of MMP (Supplementary Fig. S7D). While AZD5904 treatment seemed to affect murine $CD45^+$ cell viability in the spleen, its effect observed in combination was primarily driven by AraC toxicity (Supplementary Fig. S7E and S7F). On the basis of these results, targeting MPO *in vivo* impairs ROS homeostasis and mitochondrial function through the elevation of oxidative DNA damages and enhances cytotoxic effect of AraC treatment (Fig. 5M).

Discussion

In summary, we have demonstrated that AML cells from patients who are high responder *in vivo express* a lower level of MPO and produce a large amount of mtROS (superoxide anions) upon AraC therapy compared with low AraC responder *in vivo*. Using *in vivo* and *in vitro* models, we showed that inhibition of MPO function increases mtROS content. This elevated level of mtROS induces major oxidative damages that further affect mitochondrial redox balance and mitochondrial metabolism, leading to the sensitization of resistant cells to AraC treatment. Recently, Di Marcantonio and colleagues have suggested that increase in mtROS might be a significant therapeutic potential mediated by protein kinase PKCε in AML (59). In the following mechanistic step, mitochondrial dysfunction and oxidative stress lead to loss of the redox-sensing function of ATM (60). Consequently, the absence of redox-sensing function of ATM disrupts ROS homeostasis from mitochondria to increase cytosolic antioxidant defenses. Consistent with these observations, our study has demonstrated that MPO inhibition induces overproduction of mtROS and overexpression of ATM, which subsequently result in ROS accumulation and elevated rate of oxidative damage. Several studies have demonstrated that chemotherapeutic treatments lead to increased OxPHOS metabolism and ROS generation in residual AML cells (17) or other cancer/leukemia types (21, 47). Here, we showed that MPO level is positively correlated with mitochondrial oxygen consumption and OxPHOS gene signature, while negatively associated to mtROS generation and oxidative damage. Interestingly, it has been shown that MPO expression is negatively correlated to disease-free survival (DFS) in AML patient samples treated with standard therapy (61). However, the authors have studied the DFS in patients who had received a conventional "7+3″ therapy regimen with a combination of AraC and anthracycline, while we used AraC alone in this study. This "7+3″ combination has likely different impact on MPO expression, redox homeostasis, and mitochondrial energetics compared with a treatment with AraC alone (22). On the basis of these results, cytosolic (H_2O_2) and mitochondrial ($O_2^{\bullet-}$) ROS levels in chemoresistant cells are increased but this amount is not enough to induce the cell death. This redox imbalance has been shown to be indispensable for proliferation of resistant cancer cells. Oxidative stress is defined as an overproduction of ROS and/or the consequence of redox balance impairment. Furthermore, ROS are a large family of various molecules combining reactive species [e.g., superoxide anion radical ($O_2^{\bullet-}$) and hydroxyl radical ($HO^{\bullet}$)], nonradicals [e.g., H_2O_2 and singlet oxygen ($^1O_2$)], or adduct products (e.g., HOCl and $ONOO^-$) with many functions including second messengers and signaling. While HOCl is highly reactive, its half-life is very short, leading to an efficient and rapid pathway of H_2O_2 detoxification. In this context, MPO is also generating ROS biomarkers. Finally, every signals and stresses that increase ROS production, more specifically mtROS in our case (such as mtROS inducers) might increase above the ROS threshold priming these cells to apoptosis and finally selectively overcome the resistance to AraC by induction of DNA damage and apoptosis. Moreover and according to our finding, MPO has a new function in regulating cytosol and mtROS balance and mitochondrial energy metabolism in AML (Fig. 5M) in addition to its canonical role in inflammation and differentiation. Consistent with our results, Adane and colleagues reported that rewiring the redox metabolism, more specifically NADPH oxidase, affect core energy metabolism pathways and eventually alters differentiation in myeloid

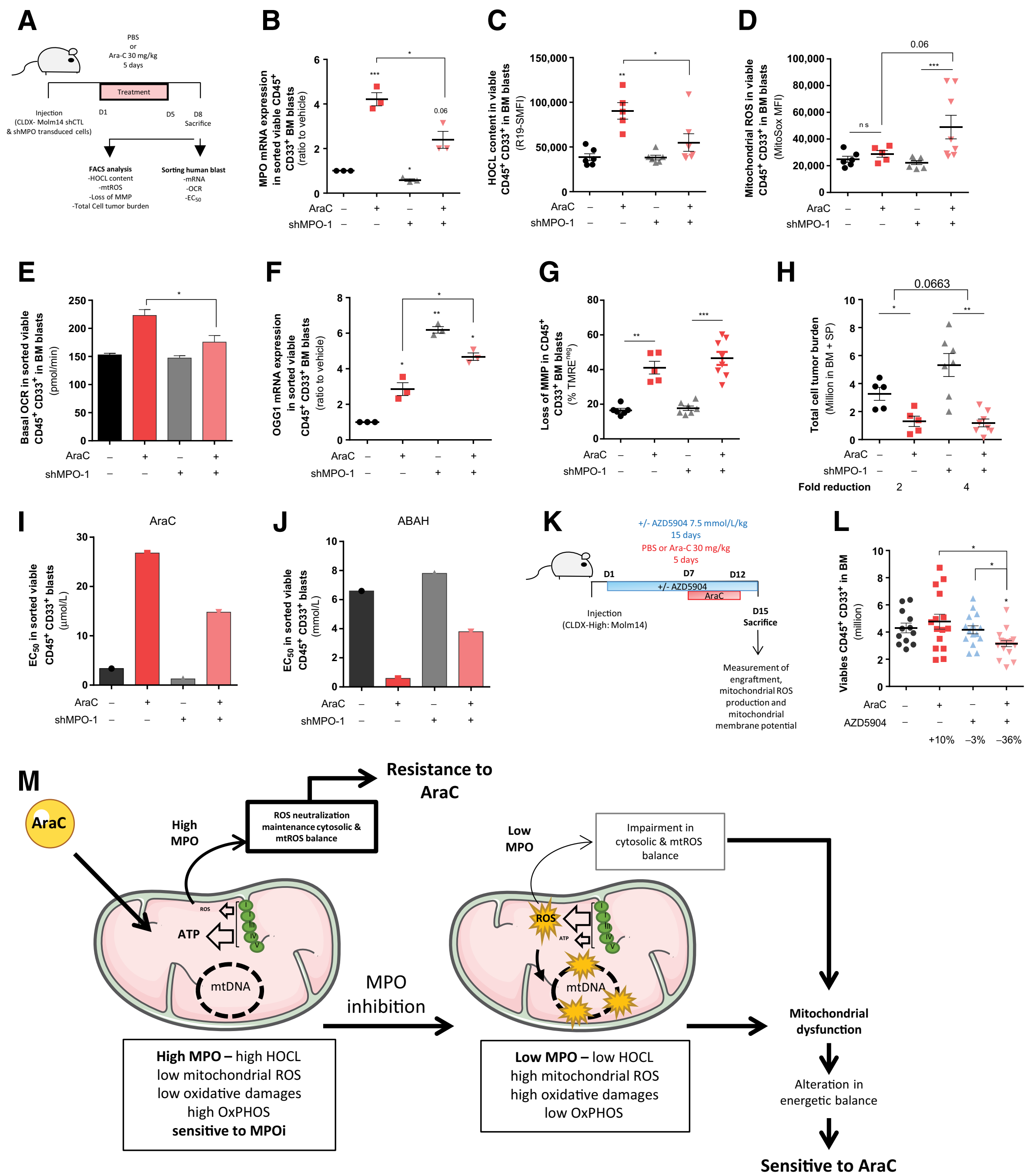

Figure 5.

In vivo targeting of MPO expression upon AraC treatment increases mtROS and oxidative DNA damages in cytarabine-resistant AML cells. **A,** Experimental design of the chemotherapy treatment used *in vivo* in AML cell line–xenografted mice. **B,** *MPO* mRNA expression was quantified in viable human-sorted AML cells from AraC- versus vehicle (PBS)-treated mice xenografted with shCtrl versus shMPO MOLM14 AML cells. **C** and **D,** mtROS and total HOCl content were measured by MitoSox and R-19S in shCtrl and shMPO human viable (Annexin V^-/7-AAD$^-$) $CD45^+CD33^+$ AML cells from AraC- versus vehicle (PBS)-treated AML-xenografted mice. **E,** ATP-linked OCR was quantified in viable human-sorted shCtrl and shMPO (Annexin V^-/7-AAD$^-$) cells from AraC- versus vehicle (PBS)-treated AML-xenografted mice. **F,** mRNA level for OGG1 was measured in human viable-sorted cells. Quantification of loss of mitochondrial membrane potential (**G**) and viability (**H**) in human shCtrl versus shMPO-transduced cells. Human residual AML cells sorted from mice BM were treated *ex vivo* with AraC (**I**) and ABAH (**J**) for 24 hours and its EC_{50} was calculated and compared with EC_{50} from matched PBS-treated AML cells. **K,** Experimental design of the chemotherapy treatment using MPO inhibitor (AZD5904) alone or in combination with AraC *in vivo* in AML cell line–xenografted mice model. **L,** Viability of AML blasts in MOLM14-xenografted mice BM upon vehicle, MPO inhibitor (AZD5904), AraC, and combination *in vivo.* **M,** Schematic diagram of mechanism of action of MPO in AML cells post-AraC. Graphs of mean ± SEM. *P* values were determined by Welch correction test (**A–J**). n.s., not significant; *, $P \leq 0.05$; **, $P \leq 0.01$; ***, $P \leq 0.001$.

precursor cells (62). Considering all these aspects, we believe that MPO could be considered as a promising new target to further enhance the efficacy of AraC chemotherapy especially during consolidation cycles with AraC alone in AML patient samples.

Disclosure of Potential Conflicts of Interest

No potential conflicts of interest were disclosed.

Authors' Contributions

Conception and design: M. Hosseini, H.R. Rezvani, M. Piechaczyk, C. Récher, J.-E. Sarry
Development of methodology: M. Hosseini, C. Bosc, T. Farge, E. Saland, C. Récher
Acquisition of data (provided animals, acquired and managed patients, provided facilities, etc.): M. Hosseini, N. Aroua, C. Bosc, T. Farge, E. Saland, S. Zaghdoudi, C. Larrue, M. Sabatier, P.L. Mouchel, M. Gotanègre, C. Récher
Analysis and interpretation of data (e.g., statistical analysis, biostatistics, computational analysis): M. Hosseini, H.R. Rezvani, N. Aroua, T. Farge, E. Saland, P.L. Mouchel, C. Récher, J.-E. Sarry
Writing, review, and/or revision of the manuscript: M. Hosseini, H.R. Rezvani, M. Piechaczyk, G. Bossis, C. Récher, J.-E. Sarry
Administrative, technical, or material support (i.e., reporting or organizing data, constructing databases): M. Hosseini, N. Aroua, T. Farge, V. Guyonnet-Dupérat, L. Jarrou, M. Gotanègre
Study supervision: J.-E. Sarry

Acknowledgments

We thank Audrey Sarry, Dr. Lucille Stuani, Dr. Nizar Serhan, all members of mice core facilities (UMS006, ANEXPLO, Inserm, Toulouse) for their support and technical assistance, and Véronique De Mas and Eric Delabesse for the management of the Biobank BRC-HIMIP (Biological Resources Centres-INSERM Midi-Pyrénées "Cytothèque des hémopathies malignes") that is supported by CAPTOR (Cancer Pharmacology of Toulouse-Oncopole and Région). We thank the flow cytometry core facility of U1048-I2MC for technical assistance, and Anne-Marie Benot, Muriel Serthelon, and Stéphanie Nevouet for their daily help about the administrative and financial management of our Team RESISTAML. The authors also thank Drs. M.A. Selak and N. Skuli for critical reading of the article. This work was supported by grants from the French government under the program "Investissement d'avenir" CAPTOR (ANR-11-PHUC-001), the Labex TOUCAN and the project ROSAML (INCA-2015-143), from the Fondation Toulouse Cancer Santé, the Fondation ARC, the Ligue National de Lutte Contre le Cancer, and from the Association G.A.E.L.

The costs of publication of this article were defrayed in part by the payment of page charges. This article must therefore be hereby marked *advertisement* in accordance with 18 U.S.C. Section 1734 solely to indicate this fact.

Received February 15, 2019; revised May 29, 2019; accepted July 19, 2019; published first July 29, 2019.

References

1. Döhner H, Weisdorf DJ, Bloomfield CD. Acute myeloid leukemia. N Engl J Med 2015;373:1136–52.
2. Lagadinou ED, Sach A, Callahan K, Rossi RM, Neering SJ, Minhajuddin M, et al. BCL-2 inhibition targets oxidative phosphorylation and selectively eradicates quiescent human leukemia stem cells. Cell Stem Cell 2013;12: 329–41.
3. Sánchez-Mendoza SE, Rego EM. Targeting the mitochondria in acute myeloid leukemia. Appl Cancer Res 2017;37:22.
4. Reiter K, Polzer H, Krupka C, Maiser A, Vick B, Rothenberg-Thurley M, et al. Tyrosine kinase inhibition increases the cell surface localization of FLT3-ITD and enhances FLT3-directed immunotherapy of acute myeloid leukemia. Leukemia 2018;32:313–22.
5. Cruijsen M, Lübbert M, Wijermans P, Huls G. Clinical results of hypomethylating agents in AML Treatment. J Clin Med 2014;4:1–17.
6. Tsai HC, Li H, Van Neste L, Cai Y, Robert C, Rassool FV, et al. Transient low doses of DNA-demethylating agents exert durable antitumor effects on hematological and epithelial tumor cells. Cancer Cell 2012;21:430–46.
7. Garcia JS, Stone RM. The development of FLT3 inhibitors in acute myeloid leukemia. Hematol Oncol Clin North Am 2017;31:663–80.
8. Hospital MA, Green AS, Maciel TT, Moura IC, Leung AY, Bouscary D, et al. FLT3 inhibitors: clinical potential in acute myeloid leukemia. Onco Targets Ther 2017;10:607–15.
9. Intlekofer AM, Shih AH, Wang B, Nazir A, Rustenburg AS, Albanese SK, et al. Acquired resistance to IDH inhibition through trans or cis dimer-interface mutations. Nature 2018;559:125–9.
10. Deberardinis RJ, Sayed N, Ditsworth D, Thompson CB. Brick by brick: metabolism and tumor cell growth. Curr Opin Genet Dev 2008;18:54–61.
11. DeBerardinis RJ, Lum JJ, Hatzivassiliou G, Thompson CB. The biology of cancer: metabolic reprogramming fuels cell growth and proliferation. Cell Metab 2008;7:11–20.
12. Vander Heiden MG, DeBerardinis RJ. Understanding the intersections between metabolism and cancer biology. Cell 2017;168:657–69.
13. Green DR, Galluzzi L, Kroemer G. Metabolic control of cell death. Science 2014;345:1250256.
14. Glasauer A, Chandel NS. Targeting antioxidants for cancer therapy. Biochem Pharmacol 2014;92:90–101.
15. Hamanaka RB, Glasauer A, Hoover P, Yang S, Blatt H, Mullen AR, et al. Mitochondrial reactive oxygen species promote epidermal differentiation and hair follicle development. Sci Signal 2013;6:ra8.
16. DeBerardinis RJ, Chandel NS. Fundamentals of cancer metabolism. Sci Adv 2016;2:e1600200.
17. Farge T, Saland E, De Toni F, Aroua N, Hosseini M, Perry R, et al. Chemotherapy-resistant human acute myeloid leukemia cells are not enriched for leukemic stem cells but require oxidative metabolism. Cancer Discov 2017;7:716–35.
18. Hosseini M, Dousset L, Mahfouf W, Serrano-Sanchez M, Redonnet-Vernhet I, Mesli S, et al. Energy metabolism rewiring precedes UVB-induced primary skin tumor formation. Cell Rep 2018;23: 3621–34.
19. Vander Heiden MG, DeBerardinis RJ. Understanding the intersections between metabolism and cancer biology. Cell 2017;168:657–69.
20. Galluzzi L, Pietrocola F, Levine B, Kroemer G. Metabolic control of autophagy. Cell 2014;159:1263–76.
21. Lee K, Giltnane JM, Balko JM, Schwarz LJ, Guerrero-Zotano AL, Hutchinson KE, et al. MYC and MCL1 cooperatively promote chemotherapy-resistant breast cancer stem cells via regulation of mitochondrial oxidative phosphorylation. Cell Metab 2017;26:633–647.
22. Bosc C, Selak MA, Sarry JE. Resistance is futile: targeting mitochondrial energetics and metabolism to overcome drug resistance in cancer treatment. Cell Metab 2017;26:705–7.
23. Diehn M, Cho RW, Lobo NA, Kalisky T, Dorie MJ, Kulp AN, et al. Association of reactive oxygen species levels and radioresistance in cancer stem cells. Nature 2009;458:780–3.
24. Cole A, Wang Z, Coyaud E, Voisin V, Gronda M, Jitkova Y, et al. Inhibition of the mitochondrial protease ClpP as a therapeutic strategy for human acute myeloid leukemia. Cancer Cell 2015;27:864–76.
25. Sriskanthadevan S, Jeyaraju DV, Chung TE, Prabha S, Xu W, Skrtic M, et al. AML cells have low spare reserve capacity in their respiratory chain that renders them susceptible to oxidative metabolic stress blood. 2015;125: 2120–30.
26. Zhou D, Shao L, Spitz DR. Reactive oxygen species in normal and tumor stem cells. Adv Cancer Res 2014;122:1–67.
27. Hachiya M, Osawa Y, Akashi M. Role of TNFα in regulation of myeloperoxidase expression in irradiated HL60 promyelocytic cells. Biochim Biophys Acta 2000;1495:237–49.
28. Silvescu CI, Sackstein R. G-CSF induces membrane expression of a myeloperoxidase glycovariant that operates as an E-selectin ligand on human myeloid cells. Proc Natl Acad Sci U S A 2014;111: 10696–701.
29. Kim Y, Yoon S, Kim SJ, Kim JS, Cheong JW, Min YH, et al. Myeloperoxidase expression in acute myeloid leukemia helps identifying patients to benefit from transplant. Yonsei Med J 2012;53:530–6.

30. Loria V, Dato I, Graziani F, Biasucci LM. Myeloperoxidase: a new biomarker of inflammation in ischemic heart disease and acute coronary syndromes. Mediators Inflamm 2008;2008:1–4.
31. Saland E, Boutzen H, Castellano R, Pouyet L, Griessinger E, Larrue C, et al. A robust and rapid xenograft model to assess efficacy of chemotherapeutic agents for human acute myeloid leukemia. Blood Cancer J 2015;5:e297. doi: 10.1038/bcj.2015.19.
32. Cen J, Zhang L, Liu F, Zhang F, Ji BS. Long-term alteration of reactive oxygen species led to multidrug resistance in MCF-7 cells. Oxid Med Cell Longev 2016;2016:7053451.
33. Brunetti L, Gundry MC, Sorcini D, Guzman AG, Huang YH, Ramabadran R, et al. Mutant NPM1 maintains the leukemic state through HOX expression. Cancer Cell 2018;34:499–512.
34. Verhaak RG, Wouters BJ, Erpelinck CA, Abbas S, Beverloo HB, Lugthart S, et al. Prediction of molecular subtypes in acute myeloid leukemia based on gene expression profiling. Haematologica 2009;94:131–4.
35. Metzeler KH, Hummel M, Bloomfield CD, Spiekermann K, Braess J, Sauerland M-C, et al. An 86-probe-set gene-expression signature predicts survival in cytogenetically normal acute myeloid leukemia. Blood 2008; 112:4193–201.
36. Nakazato T, Sagawa M, Yamato K, Xian M, Yamamoto T, Suematsu M, et al. Myeloperoxidase is a key regulator of oxidative stress mediated apoptosis in myeloid leukemic cells. Clin Cancer Res 2007;13:5436–45.
37. Kim YR, Eom JI, Kim SJ, Jeung HK, Cheong JW, Kim JS, et al. Myeloperoxidase expression as a potential determinant of parthenolide-induced apoptosis in leukemia bulk and leukemia stem cells. J Pharmacol Exp Ther 2010;335:389–400.
38. Hole PS, Darley RL, Tonks A. Do reactive oxygen species play a role in myeloid leukemias? Blood 2011;117:5816–26.
39. Mondet J, Lo Presti C, Garrel C, Skaare K, Mariette C, Carras S, et al. *De novo* adult acute myeloid leukemia patients display at diagnosis functional deregulation of redox balance correlated with molecular subtypes and overall survival. Haematologica 2019 Feb 28 [Epub ahead of print].
40. Matés JM, Segura JA, Alonso FJ, Márquez J. Oxidative stress in apoptosis and cancer: an update. Arch Toxicol 2012;86:1649–65.
41. Prieto-Bermejo R, Romo-González M, Pérez-Fernández A, Ijurko C, Hernández-Hernández Á. Reactive oxygen species in haematopoiesis: leukaemic cells take a walk on the wild side. J Exp Clin Cancer Res 2018;37:125.
42. Bossis G, Sarry JE, Kifagi C, Ristic M, Saland E, Vergez F, et al. The ROS/SUMO axis contributes to the response of acute myeloid leukemia cells to chemotherapeutic drugs. Cell Rep 2014;7:1815–23.
43. Okon IS, Zou MH. Mitochondrial ROS and cancer drug resistance: implications for therapy. Pharmacol Res 2015;100:170–4.
44. Sabharwal SS, Schumacker PT. Mitochondrial ROS in cancer: initiators, amplifiers or an Achilles' heel? HHS public access. Nat Rev Cancer 2014;14: 709–21.
45. Liemburg-Apers DC, Willems PH, Koopman WJ, Grefte S. Interactions between mitochondrial reactive oxygen species and cellular glucose metabolism. Arch Toxicol 2015;89:1209–26.
46. Wang H, Gao Z, Liu X, Agarwal P, Zhao S, Conroy DW, et al. Targeted production of reactive oxygen species in mitochondria to overcome cancer drug resistance. Nat Commun 2018;9:562.
47. Kuntz EM, Baquero P, Michie AM, Dunn K, Tardito S, Holyoake TL, et al. Targeting mitochondrial oxidative phosphorylation eradicates therapy-resistant chronic myeloid leukemia stem cells. Nat Med 2017;23: 1234–40.
48. Galvan DL, Green NH, Danesh FR. The hallmarks of mitochondrial dysfunction in chronic kidney disease. Kidney Int 2017;92:1051–7.
49. Fu X, Liu W, Huang Q, Wang Y, Li H, Xiong Y, et al. Targeting mitochondrial respiration selectively sensitizes pediatric acute lymphoblastic leukemia cell lines and patient samples to standard chemotherapy. Am J Cancer Res 2017;7:2395–405.
50. Gibellini L, Pinti M, Nasi M, De Biasi S, Roat E, Bertoncelli L, et al. "Interfering with ROS metabolism in cancer cells: the potential role of quercetin." Cancers 2010;2:1288–1311.
51. Guzman ML, Rossi RM, Karnischky L, Li X, Peterson DR, Howard DS, et al. The sesquiterpene lactone parthenolide induces apoptosis of human acute myelogenous leukemia stem and progenitor cells. Blood 2005;105: 4163–9.
52. Pei S, Minhajuddin M, Callahan KP, Balys M, Ashton JM, Neering SJ, et al. Targeting aberrant glutathione metabolism to eradicate human acute myelogenous leukemia cells. J Biol Chem 2013;288:33542–58.
53. Han Y, Chen JZ. Oxidative stress induces mitochondrial DNA damage and cytotoxicity through independent mechanisms in human cancer cells. Biomed Res Int 2013;2013:825065.
54. Markkanen E. Not breathing is not an option: How to deal with oxidative DNA damage. DNA Repair 2017;59:82–105.
55. Scott TL, Rangaswamy S, Wicker CA, Izumi T. Repair of oxidative DNA damage and cancer: recent progress in DNA base excision repair. Antioxid Redox Signal 2014;20:708–26.
56. Rezvani HR, Mazurier F, Cario-André M, Pain C, Ged C, Taïeb A, et al. Protective effects of catalase overexpression on UVB-induced apoptosis in normal human keratinocytes. J Biol Chem 2006;281:17999–8007.
57. Hosseini M, Mahfouf W, Serrano-Sanchez M, Raad H, Harfouche G, Bonneu M, et al. Premature skin aging features rescued by inhibition of NADPH oxidase activity in XPC-deficient mice. J Invest Dermatol 2015; 135:1108–18.
58. Nissanka N, Moraes CT. Mitochondrial DNA damage and reactive oxygen species in neurodegenerative disease. FEBS Lett 2018;592: 728–42.
59. Di Marcantonio D, Martinez E, Sidoli S, Vadaketh J, Nieborowska-Skorska M, Gupta A, et al. Protein kinase C epsilon is a key regulator of mitochondrial redox homeostasis in acute myeloid leukemia. Clin Cancer Res 2018; 24:608–18.
60. Zhang Y, Lee JH, Paull TT, Gehrke S, D'Alessandro A, Dou Q, et al. Mitochondrial redox sensing by the kinase ATM maintains cellular antioxidant capacity. Sci Signal 2018;11:eaaq0702.
61. Matsuo T, Kuriyama K, Miyazaki Y, Yoshida S, Tomonaga M, Emi N, et al. The percentage of myeloperoxidase-positive blast cells is a strong independent prognostic factor in acute myeloid leukemia, even in the patients with normal karyotype. Leukemia 2003;17:1538–43.
62. Adane B, Ye H, Khan N, Pei S, Minhajuddin M, Stevens BM, et al. The hematopoietic oxidase NOX2 regulates self-renewal of leukemic stem cells. Cell Rep 2019;27:238–54.